AGU PUBLICATIONS

JGR

Journal of Geophysical Research: Space Physics

RESEARCH ARTICLE

10.1002/2014JA020688

**Key Points:**

- Report on a transient small-scale auroral structure at Jupiter
- Its magnetospheric source is fixed in local time (noon)
- Plausible explanation: inward plasma flow in the equatorial plane

**Supporting Information:**

- Text S1 and Figure S1
- Animation S1
- Animation S2

**Correspondence to:**
B. Palmaerts,
benjamin.palmaerts@doct.ulg.ac.be

**Citation:**
Palmaerts, B., A. Radioti, D. Grodent, E. Chané, and B. Bonfond (2014), Transient small-scale structure in the main auroral emission at Jupiter, *J. Geophys. Res. Space Physics*, *119*, 9931–9938, doi:10.1002/2014JA020688.

Received 6 OCT 2014
Accepted 1 DEC 2014
Accepted article online 3 DEC 2014
Published online 17 DEC 2014

# Transient small-scale structure in the main auroral emission at Jupiter

**B. Palmaerts[1,2], A. Radioti[1], D. Grodent[1], E. Chané[3], and B. Bonfond[1]**

[1]Laboratoire de Physique Atmosphérique et Planétaire, Université de Liège, Liège, Belgium, [2]Max-Planck-Institut für Sonnensystemforschung, Göttingen, Germany, [3]Centre for mathematical Plasma Astrophysics, Leuven, Belgium

**Abstract** The main auroral emission at Jupiter results from the ionosphere-magnetosphere coupling current system associated with the corotation breakdown of iogenic plasma in the current sheet. The morphology and brightness of the main auroral emission are generally suggested to be stable during time intervals of the order of an hour. Here we reveal a transient small-scale structure in the main emission that is characterized by a localized brightness enhancement close to noon local time. The evolution of this small-scale structure is investigated in both hemispheres on the basis of far UV images obtained with the Hubble Space Telescope between 1997 and 2007. Our observations indicate that the transient feature vary within a few tens of minutes. As one plausible explanation based on Galileo observations, we suggest that the localized enhancement of the field-aligned currents associated with the transient structure is due to the shear induced by intermittent inward plasma flow near noon in the equatorial plane.

## 1. Introduction

The main auroral emission at Jupiter is generally suggested to be related to the magnetosphere-ionosphere coupling current system associated with the breakdown of rigid corotation in the equatorial plane between 15 and 40 $R_J$ [e.g., *Cowley and Bunce*, 2001, 2003; *Hill*, 2001; *Nichols and Cowley*, 2004]. Plasma coming from the ionization of the neutral gas supplied by the volcanic activity on Io diffuses outward in the equatorial plane, and by conservation of the angular momentum, its angular velocity steadily decreases. When the plasma angular velocity becomes lower than that of the neutral atmosphere, ion-neutral collisions in the Pedersen layer of the ionosphere provide a frictional torque on the feet of the field lines which acts to spin the plasma back up toward rigid corotation. This torque is then communicated to the equatorial plasma by a large-scale electric current system. The $\mathbf{j} \times \mathbf{B}$ forces ($\mathbf{j}$ and $\mathbf{B}$ represent the current density and the magnetic field, respectively) of the equatorial radial current tend to accelerate the equatorial plasma toward corotation. As these forces are not strong enough to sustain the plasma acceleration up to corotation, a breakdown of corotation occurs. The field-aligned currents of the corotation enforcement current system flow from the ionosphere to the equatorial plane (upward currents) in the inner part and return (downward currents) in the outer part [see *Cowley and Bunce*, 2001, Figure 1]. The upward currents are carried by downward moving electrons precipitating in the ionosphere and producing auroral emissions.

The main auroral emission forms a relatively steady strip of emission around the magnetic pole whose general morphology remains roughly stable, even over time periods spanning several years, and is fixed in System III longitudes [*Grodent et al.*, 2003]. Hubble Space Telescope (HST) observations revealed that the main emission cones around the spin axis at the planetary rotation rate owing to the tilted dipole and exhibits temporal variations on timescales of a few hours and occasional dramatic enhancements in the dawn sector which last tens of minutes [*Gérard et al.*, 1994; *Ballester et al.*, 1996; *Grodent et al.*, 2003; *Gustin et al.*, 2006]. The main UV auroral emission at Jupiter is estimated to contribute 75% of the Jovian auroral brightness integrated over high latitudes [*Nichols et al.*, 2009]. Additionally, the main auroral emission brightness was observed to be correlated with the solar wind pressure [*Nichols et al.*, 2007, 2009; *Clarke et al.*, 2009]. Furthermore, *Grodent et al.* [2008a] showed that the location of the main emission could change by up to 3° of latitude over long periods of time. Alternatively to the explanation involving variations of solar wind conditions, they explained this latitudinal shift by internal variations of the current sheet parameters. Similarly, *Bonfond et al.* [2012] showed that the main oval emission continuously expanded over a few months in spring 2007 and they attributed these temporal changes to internal variations triggered by Io's volcanic activity.

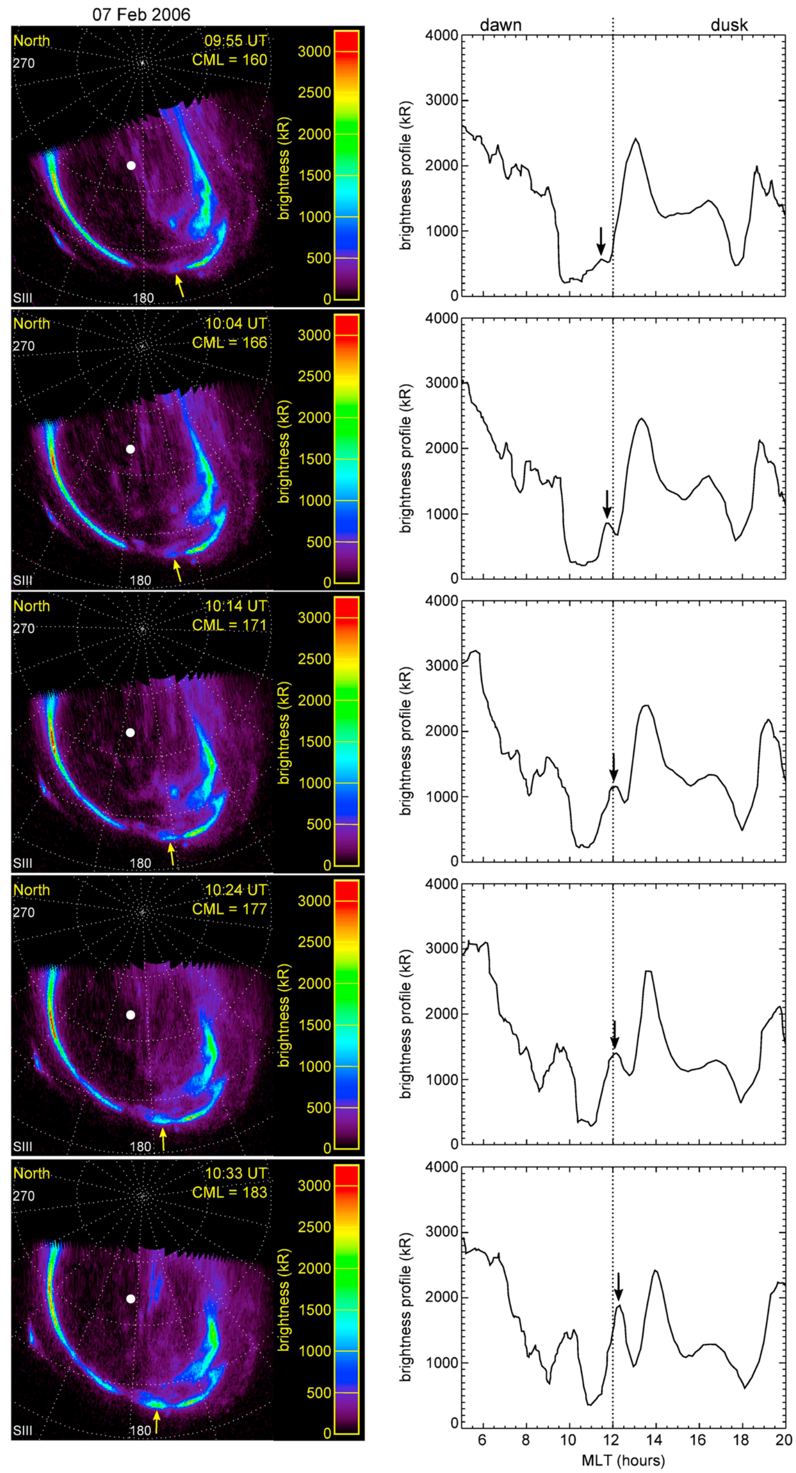


**Figure 1.** (left column) Sequence of five polar projections in System III polar coordinate system (white small dots) of HST-ACS auroral images at the north pole of Jupiter. System III 180° meridian is oriented toward the bottom of the page. The images were taken on 7 February 2006. The time of observation and the CML for each image are indicated in the right upper corner of each projection. The observation sequence lasts for 38 min and CML ranges from 160 to 183°. The white large dot indicates the morphological center of the main emission ($\lambda_{III} = 186°$ and $\phi = 74°$). (right column) Profiles of the maximum brightness along the main emission corresponding to the projections (left). The brightness is given in kilorayleighs (above the background emission) as a function of the magnetic local time derived from the magnetic field mapping of *Vogt et al.* [2011]. The dotted line indicates the magnetic noon. An arrow points to the localized peak which corresponds to a transient auroral feature in the main emission.

Apart from temporal variations, observations at various central meridian longitudes (CMLs) in the northern and the southern hemispheres have shown that the main emission morphology varies with the magnetic local time [*Grodent et al*., 2003]: the dawn to noon portion forms a narrow arc while the noon to dusk portion is usually broader and less structured. Furthermore, in the northern hemisphere, a localized magnetic anomaly, fixed in SIII coordinates, influences the main emission shape [*Grodent et al*., 2008b]. Analysis of HST images revealed the presence of a discontinuity in the main emission, where the brightness significantly drops [*Radioti et al*., 2008]. It was shown that the discontinuity is present in both hemispheres and fixed in magnetic local time between 08:00 and 13:00 magnetic local time (MLT). Based on in situ observations and magnetohydrodynamic (MHD) simulations, the authors suggested that the origin of this feature is associated with the presence of reduced upward and/or downward field-aligned currents in that region. Recent MHD simulations addressed the local time discontinuity in the main emission [*Chané et al*., 2013]. They suggested that an asymmetry in the thermal pressure distribution, due to the interaction between the rotating plasma and the magnetopause, decreases the strength of the corotation enforcing current system and thus results in the formation of a discontinuity in the main emission in the prenoon to noon sector.

In the present study, we identify for the first time a transient small-scale structure in the main emission which appears close to magnetic noon and we investigate its dynamic evolution in both hemispheres.

## 2. Observations of a Small-Scale Structure in the Main Auroral Emission

This study is based on the analysis of the observations collected by the HST between 1997 and 2007. Images of the auroral emissions were obtained with the Space Telescope Imaging Spectrograph (STIS) and the Advanced Camera for Surveys (ACS). A dark count subtraction was applied to images as well as geometric and photometric corrections. Data reduction procedures are described by *Grodent et al*. [2003]. We removed an empirical planetary disk background following the method described by *Bonfond et al*. [2011]. We used conversion factors computed by *Gustin et al*. [2012] for each filter, assuming a typical color ratio of 2.5 [*Gérard et al*., 2002; *Gustin et al*., 2004], to convert observed count rates into kilorayleighs. HST images are projected on a polar map fixed in System III which facilitates the detection of features corotating with the planet, leading or lagging corotation. This orthographic projection required a limb fitting procedure to determine the center position of the planet, as described by *Bonfond et al*. [2009]. The altitude of the auroral emissions considered for the projections is 250 km [*Vasavada et al*., 1999].

Figure 1 (left column) shows a sequence of five polar projections in SIII of FUV auroral images of the north pole of Jupiter, taken on 7 February 2006 by HST-ACS. The observation sequence, made of 17 images, lasts for 38 min (see Animation S1 in the supporting information). Here we show five of them acquired ~10 min apart. During this sequence the central meridian longitude (CML) of the planet changes from 160° to 183°. The right column shows the peak brightness along the main emission as a function of the magnetic local time in kilorayleighs (kR) above the background emission. In order to plot the profiles, we used radial cuts in the projections, starting from the morphological center of the main emission. This central position was derived geometrically [*Grodent et al*., 2004] and is independent of any magnetic field model. It is located in longitude $\lambda_{III} = 186°$ and latitude $\phi = 74°$ for northern aurora and $\lambda_{III} = 32°$ and latitude $\phi = -82°$ for southern aurora. It is indicated by a white large dot on the polar projections. The magnetic local time corresponding to the location of the peak of the main emission in the profiles is derived using the magnetic field model of *Vogt et al*. [2011]. In this section, mentioned local time always refers to the magnetic local time.

Local time variations of the main emission are readily identifiable on the projected auroral images as well as on the corresponding profiles. In all panels, the brightness of the main emission smoothly decreases with local time until the prenoon sector (~9:00 to 12:00 MLT) where intensity suddenly drops to a minimum value, forming a discontinuity [*Radioti et al*., 2008]. In the afternoon sector, there is a persistent peak in the profile near 14:00 MLT, whereas the intensity drops at dusk before rising again. While the morphology and brightness of the main emission are relatively stable during the 38 min interval, a small-scale feature in the main emission is continuously growing close to noon (indicated by an arrow in Figure 1). At the end of the sequence (within 38 min), the brightness of the feature becomes remarkably high, corresponding to 1.5 times the mean brightness of the main emission (~ 1300 kR), whereas it was roughly half the mean brightness at the start of the sequence. The feature was growing with a mean rate of 39 kR/min during this 38 min long sequence. It should be noted that the local time region where it is observed is little affected by limb brightening effects, contrary to the early dawn and late dusk sectors [*Grodent et al*., 1997]. Therefore, this constant brightness increase does not result from an observing geometry effect.

Figure 2 shows a 38 min long sequence of polar projections of auroral emissions in the southern hemisphere acquired on 11 March 2007 by HST-ACS (see Animation S2). A total of 19 images were obtained, but we show only five of them acquired every ~10 min (CML increases from 278° to 301°). Projections are displayed as if the aurora was seen from above the north pole through the planet. The dark line crossing images is caused by a bad anode on the ACS/SBC MAMA (Solar Blind Channel Multi-Anode Microchannel Array) detector that disables some pixel rows. The intensity of the main emission varies with local time: the emission is much more intense on the duskside than on the dawnside. The brightness reaches its minimum value in the prenoon sector, i.e., in the region where the discontinuity of the main emission is usually located [*Radioti et al*., 2008]. While the overall main emission brightness remains globally stable during the 38 min interval as it was in the north, close to the discontinuity, at ~12:00 MLT, a feature emerges (Figure 2, left column). It corresponds to a localized peak in the intensity profile which is gradually increasing with a mean growth rate of 12 kR/min, ~3 times slower compared to the previous case in the northern hemisphere.

The two examples of a small-scale transient structure discussed above are not exceptional cases. We observe a similar localized peak close to noon in ~60% of the HST auroral images acquired between 1997 and 2007 (for a total of 1685 images). In addition to considering individual images, we also examine observation sequences made of a minimum of four contiguous images during an HST observation orbit. In 60 out of 80 sequences, we observe the small-scale structure in at least one image but not necessarily throughout the whole sequence. That highlights the transient nature of this structure. The brightness enhancement evolves within a few tens of minutes, increasing or decreasing over the observed sequences. Some observations demonstrate that the localized peak can evolve into two separate features. Hence, the transient small-scale feature is regularly observed in both hemispheres. Its magnetospheric source is relatively fixed in local time, and it is located around magnetic noon. Whereas the main emission is considered to be relatively stable [*Grodent et al*., 2003], we show that a small-scale dynamic feature over timescales of an hour is conspicuous in the HST data.

The properties of the localized transient feature were statistically analyzed on the basis of 85 HST auroral images, each of them taken on a different day (53 images for the northern hemisphere and 32 images for the southern hemisphere). The CML of these images are quasi-uniformly distributed between 115° and 234° for the northern hemisphere and between 301° and 114° for the southern hemisphere. The localized small-scale feature can be 4.6 times brighter than the mean brightness along the main oval. The peak brightness of the feature can rise up to 3.1 MR (megarayleighs) but remains below 2.2 MR in ~90% out of cases in both hemispheres. In half of the cases, the feature brightness does not exceed 1.2 MR.

Figure 3 presents histograms of the position of the localized peak center in magnetic local time for the northern and the southern hemispheres, respectively. The mean magnetic longitude of the peak center is ~12:30 MLT in both hemispheres. Vertical bars correspond to the standard deviation of the number of cases, assuming that the probability of the presence of the localized intense region within a certain local time interval follows a binomial distribution. The binomial distribution describes a success/failure experiment which corresponds to the presence/absence of the small-scale structure in a local time range. The red dashed lines indicate the local time range where the feature can be found, if we account for its longitudinal width. The width of the peak is given by the full width at half maximum of the Gaussian function best fitting the brightness curve threading the feature. This width is mostly less than 1:15 in LT (~70% of the cases in the northern hemisphere and ~85% in the southern hemisphere) but can occasionally spread over 3 h in LT. The transient small-scale structure is observed in a local time region similar in both hemispheres, between 9:00 and 15:30 MLT in the northern hemisphere and 10:00 and 15:00 MLT in the southern hemisphere. Thus, it may be concluded that the equatorial source region is fixed in local time. Local time sectors covered by the discontinuity are bounded by blue dashed lines, for reference, between 8:00 and 13:00 MLT. These limits are determined by defining discontinuity as a region along the main emission where intensity drops below 40% of the mean brightness of the main emission. The small-scale feature often appears within the duskward edge of the discontinuity. Therefore, the presence of this feature might influence the apparent length of the discontinuity, which was discussed based on north–south quasi-simultaneous auroral observations [*Gérard et al*., 2013].

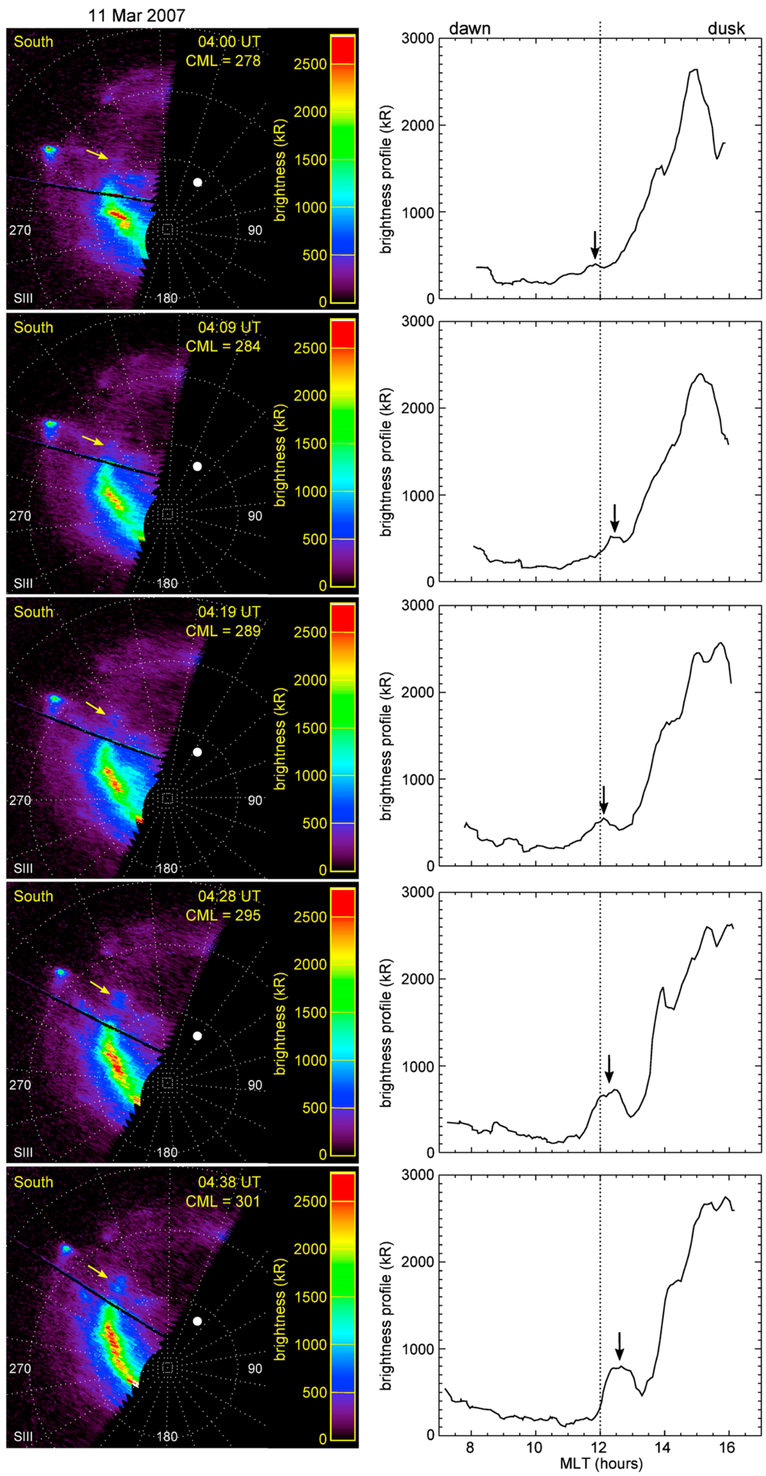


**Figure 2.** (left column) Sequence of five polar projections in System III polar coordinate system (white small dots) of HST-ACS auroral images at the south pole of Jupiter. System III 180° meridian is oriented toward the bottom of the page. Images were taken on 11 March 2007. The time of observation and the CML for each image are indicated in the right upper corner of each projection. The observation sequence lasts for 38 min, and CML ranges from 278 to 301°. The white large dot indicates the morphological center of the main emission ($\lambda_{III} = 32°$ and $\phi = -82°$). (right column) Profiles of the maximum brightness along the main emission corresponding to the projections. The brightness is given in kilorayleighs (above the background emission) as a function of the magnetic local time derived from the magnetic field mapping of *Vogt et al.* [2011]. The dotted line indicates the magnetic noon. An arrow points to the localized peak which corresponds to a transient auroral feature in the main emission.

  

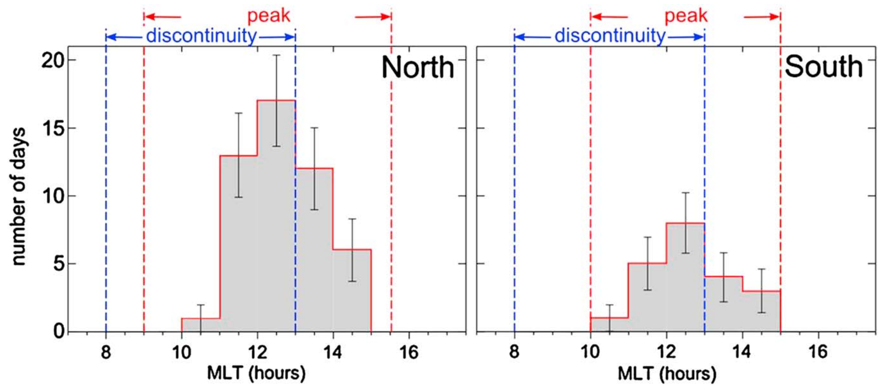


**Figure 3.** Histograms showing the local time position of the center of the small-scale structure in the (left) northern and (right) southern hemispheres. The statistical analysis is based on 53 STIS and ACS images for the northern hemisphere and 32 images for the southern hemisphere, obtained during the years 1997–2007, each of them on a different day. The deviation bars were applied according to the binomial law. The red and blue dashed lines limit the sectors covered by the peak and by the discontinuity, respectively, taking into account their longitudinal extent. The magnetic field model of *Vogt et al*. [2011] is used for the magnetic mapping.

The evolution of the transient structure is investigated by analyzing statistically the growth and decay rates of its brightness during an auroral observation sequence. These rates are obtained by performing a linear interpolation of the evolution of the peak brightness of the feature throughout the observation. We considered 18 sequences of auroral images during which the brightness of the small-scale feature continuously grows for an interval of minimum 16 min and 9 sequences during which the brightness of the feature decreases for at least 16 min. The observation sequences were selected in both hemispheres and last between 16 and 40 min. In the unconsidered sequences, the brightness of the small-scale feature varies without any particular trend. Histograms in Figure 4 present the growth and decay rates. The brightness of the feature generally changes at a rate lower than 60 kR/min while the average rates are ~29 kR/min for the growth rate and ~41 kR/min for the decay rate. The variances on these average rates are ~16 kR/min and ~19 kR/min, respectively, while the error due to measurement uncertainties ranges between ~1 and ~10 kR/min. In one case, the decay rate exceeds 80 kR/min. The feature brightness evolves with the same range of rates in both hemispheres.

## 3. Discussion

The auroral observations indicate that a transient small-scale structure close to noon is commonly observed in the main emission in both hemispheres. This points out to a localized source region in the magnetosphere

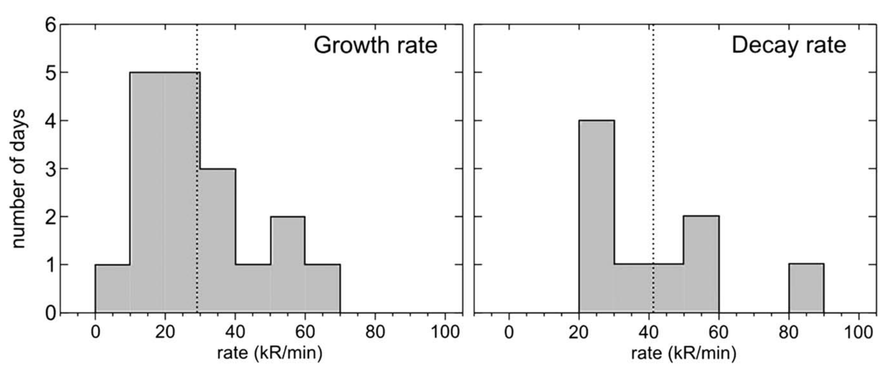


**Figure 4.** Histograms showing (left) the growth rate and (right) the decay rate of the transient small-scale feature brightness. The rates are given in kilorayleighs per minutes and are obtained by a linear interpolation of the evolution of the peak brightness of the feature. The statistical analysis is based on 27 sequences of STIS and ACS images obtained during the years 1997–2007. Only the sequences for which the brightness continuously grows or decays for an interval of minimum 16 min are considered. The dotted lines correspond to the mean growth rate and the mean decay rate, respectively.

of Jupiter. Such a transient feature should be associated with a transient increase in the density of the upward field-aligned currents close to noon.

The mean field-aligned currents inferred from Galileo observations in the equatorial plane [*Khurana*, 2001] are inconclusive regarding a localized enhancement in this local time region given that the local time sector between 13:00 and 15:00 MLT was not well sampled by Galileo at distances beyond 20 $R_J$. Moreover, the field-aligned currents estimates based on Galileo data rest on spatial and temporal averaging, and thus, they might smooth out a small-scale enhancement in the field-aligned currents density.

Observations of the plasma velocities obtained with the plasma instrumentation onboard Galileo revealed strong radial flows up to ~200 km/**s**, directed toward Jupiter in the equatorial plane around noon [*Frank and Paterson*, 2004]. These large inward radial velocities have been measured for two out of three outbound orbital segments presented in the paper (in May and in December 2000) with variability on timescales of hours (see Figure S1 in the supporting information). These flows have been observed at approximately 25 $R_J$ in a region where the measured azimuthal component of the plasma flow slows below rigid corotation and where field-aligned electron beams are observed. Hence, this region appears to correspond to the main auroral emission. *Frank and Paterson* [2004] argued that these inward plasma flows in this local time sector indicate that the influence of the solar wind extends planetward to radial distances of ~25 $R_J$, similarly to what is suggested by *Khurana* [2001]. These Galileo in situ measurements suggest the following scenario, which is compatible with our auroral observations. The possibly intermittent presence of a region of inward moving plasma would create a strong gradient in $B_z$ in the azimuthal direction due to the radial velocity shear with the surrounding plasma. Since positive azimuthal $B_z$ gradients generate radial electrical currents in the current sheet, the electrical currents responsible for the main auroral emission would increase in the local time sector where the shear induced by the inward flow are observed. This localized and intermittent enhancement in the field-aligned current density would result in a localized increase of the brightness of the main emission around noon, consistent with the observations of the transient small-scale auroral structure described in this study. In a future study, the proposed scenario could be confirmed by computing the ionospheric field-aligned currents associated with the velocity shear.

Previous studies based on MHD simulations of the Jovian magnetosphere [*Chané et al*., 2013] predicted local time asymmetries of the main auroral emission such as the presence of a discontinuity that was described by *Radioti et al*. [2008]. Further work based on these simulations indicate that localized inward plasma flow around noon in the equatorial plane generates transient enhancements of the main auroral emission in the corresponding sector, in agreement with our observations and our proposed scenario. However, an in-depth analysis of these simulations exceeds the scope of this work and is going to be presented in a future paper.

## 4. Summary and Conclusions

In this study, we identify and characterize a transient small-scale feature in the Jovian main auroral emission close to noon based on sequences of HST auroral images. Our statistical analysis shows that the feature is observed in both hemispheres, and it is relatively fixed in local time. Its location ranges between 09:00 and 15:30 MLT in the northern hemisphere and between 10:00 and 15:00 MLT in the southern hemisphere. Furthermore, its intensity can be 4.6 times larger than the mean brightness of the main emission and the average growth and decay brightness rates are ~29 kR/min and ~41 kR/min, respectively. Its local time extent generally spans less than 1.25 h but can sometimes reach up to 3 h. Our observations indicate that the main emission is not a longitudinally uniform structure and that it can vary within a few tens of minutes. As one plausible explanation, we suggest that intermittent inward plasma flow near noon in the equatorial plane is responsible for the transient small-scale structure observed in the auroral images, as the induced plasma velocity shear would lead to consistently localized field-aligned currents.

**Acknowledgments**
This work is based on observations with the NASA/ESA Hubble Space Telescope obtained at Space Telescope Science Institute (STScI, https://archive.stsci.edu/hst/search.php), which is operated by AURA, Inc., for NASA under contract NAS5-26555. This research was partly supported by the Fonds de la Recherche Scientifique (F.R.S.-FNRS) and the PRODEX Program managed by the European Space Agency in collaboration with the Belgian Federal Science Policy Office. B.B. is funded by the Fonds de la Recherche Scientifique (F.R.S.-FNRS). E.C. is funded by the Belgian Science Policy Office (IAP P7/08 CHARM) and by the Research Foundation-Flanders (FWO 12M0115N).

Larry Kepko thanks the reviewers for their assistance in evaluating this paper.

## References

Ballester, G. E., et al. (1996), Time-resolved observations of Jupiter's far ultraviolet aurora, *Science*, *274*, 409–412.

Bonfond, B., D. Grodent, J.-C. Gérard, A. Radioti, V. Dols, P. A. Delamere, and J. T. Clarke (2009), The Io UV footprint: Location, inter-spot distances and tail vertical extent, *J. Geophys. Res.*, *114*, A07224, doi:10.1029/2009JA014312.

Bonfond, B., M. F. Vogt, J.-C. Gérard, D. Grodent, A. Radioti, and V. Coumans (2011), Quasi-periodic polar flares at Jupiter. A signature of pulsed dayside reconnections?, *Geophys. Res. Lett.*, *38*, L02104, doi:10.1029/2010GL045981.

Bonfond, B., D. Grodent, J.-C. Gérard, T. Stallard, J. T. Clarke, M. Yoneda, A. Radioti, and J. Gustin (2012), Auroral evidence of Io's control over the magnetosphere of Jupiter, *Geophys. Res. Lett.*, *39*, L01105, doi:10.1029/2011GL050253.

Chané, E., J. Saur, and S. Poedts (2013), Modeling Jupiter's magnetosphere: Influence of the internal sources, *J. Geophys. Res.: Space Phys.*, *118*, 2157–2172, doi:10.1002/jgra.50258.

Clarke, J. T., et al. (2009), Response of Jupiter's and Saturn's auroral activity to the solar wind, *J. Geophys. Res.*, *114*, A05210, doi:10.1029/2008JA013694.

Cowley, S. W. H., and E. J. Bunce (2001), Origin of the main auroral oval in Jupiter's coupled magnetosphere-ionosphere system, *Planet. Space Sci.*, *49*, 1067–1088, doi:10.1016/s0032-0633(00)00167-7.

Cowley, S. W. H., and E. J. Bunce (2003), Modulation of Jupiter's main auroral oval emissions by solar wind induced expansions and compressions of the magnetosphere, *Planet. Space Sci.*, *51*, 57–79, doi:10.1016/s0032-0633(02)00118-6.

Frank, L. A., and W. R. Paterson (2004), Plasmas observed near local noon in Jupiter's magnetosphere with the Galileo spacecraft, *J. Geophys. Res.*, *109*, A11217, doi:10.1029/2002JA009795.

Gérard, J.-C., V. Dols, R. Prangé, and F. Paresce (1994), The morphology of the north Jovian ultraviolet aurora observed with the Hubble Space Telescope, *Planet. Space Sci.*, *42*, 905–917.

Gérard, J.-C., J. Gustin, D. Grodent, P. Delamere, and J. T. Clarke (2002), Excitation of the FUV Io tail on Jupiter: Characterization of the electron precipitation, *J. Geophys. Res.*, *107*(A11), 1394, doi:10.1029/2002JA009410.

Gérard, J.-C., D. Grodent, A. Radioti, B. Bonfond, and J. T. Clarke (2013), Hubble observations of Jupiter's North–South conjugate ultraviolet aurora, *Icarus*, *226*, 1559–1567, doi:10.1016/j.icarus.2013.08.017.

Grodent, D., G. R. Gladstone, J.-C. Gérard, V. Dols, and J. H. Waite (1997), Simulation of the morphology of the Jovian UV North Aurora observed with the Hubble space telescope, *Icarus*, *128*, 306–321, doi:10.1006/icar.1997.5740.

Grodent, D., J. T. Clarke, J. Kim, J. H. Waite Jr., and S. W. H. Cowley (2003), Jupiter's main auroral oval observed with HST-STIS, *J. Geophys. Res.*, *108*(A11), 1389, doi:10.1029/2003JA009921.

Grodent, D., J.-C. Gérard, J. T. Clarke, G. R. Gladstone, and J. H. Waite Jr. (2004), A possible auroral signature of magnetotail reconnection process on Jupiter, *J. Geophys. Res.*, *109*, A05201, doi:10.1029/2003JA010341.

Grodent, D., J.-C. Gérard, A. Radioti, B. Bonfond, and A. Saglam (2008a), Jupiter's changing auroral location, *J. Geophys. Res.*, *113*, A01206, doi:10.1029/2007JA012601.

Grodent, D., B. Bonfond, J.-C. Gérard, A. Radioti, J. Gustin, J. T. Clarke, J. Nichols, and J. E. P. Connerney (2008b), Auroral evidence of a localized magnetic anomaly in Jupiter's northern hemisphere, *J. Geophys. Res.*, *113*, A09201, doi:10.1029/2008JA013185.

Gustin, J., J.-C. Gérard, D. Grodent, S. W. H. Cowley, J. T. Clarke, and A. Grard (2004), Energy-flux relationship in the FUV Jovian aurora deduced from HST-STIS spectral observations, *J. Geophys. Res.*, *109*, A10205, doi:10.1029/2003JA010365.

Gustin, J., S. W. H. Cowley, J.-C. Gérard, G. R. Gladstone, D. Grodent, and J. T. Clarke (2006), Characteristics of Jovian morning bright FUV aurora from Hubble space telescope/space telescope imaging spectrograph imaging and spectral observations, *J. Geophys. Res.*, *111*, A09220, doi:10.1029/2006JA011730.

Gustin, J., B. Bonfond, D. Grodent, and J.-C. Gérard (2012), Conversion from HST ACS and STIS auroral counts into brightness, precipitated power, and radiated power for $H_2$ giant planets, *J. Geophys. Res.*, *117*, A07316, doi:10.1029/2012JA017607.

Hill, T. W. (2001), The Jovian auroral oval, *J. Geophys. Res.*, *106*(A5), 8101–8107, doi:10.1029/2000JA000302.

Khurana, K. K. (2001), Influence of solar wind on Jupiter's magnetosphere deduced from currents in equatorial plane, *J. Geophys. Res.*, *106*(A11), 25,999–26,016, doi:10.1029/2000JA000352.

Nichols, J. D., and S. W. H. Cowley (2004), Magnetosphere-ionosphere coupling currents in Jupiter's middle magnetosphere: Effect of precipitation-induced enhancement of the ionospheric Pedersen conductivity, *Ann. Geophys.*, *22*, 1799–1827, doi:10.5194/angeo-22-1799-2004.

Nichols, J. D., E. J. Bunce, J. T. Clarke, S. W. H. Cowley, J.-C. Gérard, D. Grodent, and W. R. Pryor (2007), Response of Jupiter's UV auroras to interplanetary conditions as observed by the Hubble space telescope during the Cassini flyby campaign, *J. Geophys. Res.*, *112*, A02203, doi:10.1029/2007JA012005.

Nichols, J. D., J. T. Clarke, J.-C. Gérard, D. Grodent, and K. C. Hansen (2009), Variation of different components of Jupiter's auroral emission, *J. Geophys. Res.*, *114*, A06210, doi:10.1029/2009JA014051.

Radioti, A., J.-C. Gérard, D. Grodent, B. Bonfond, N. Krupp, and J. Woch (2008), Discontinuity in Jupiter's main auroral oval, *J. Geophys. Res.*, *113*, A01215, doi:10.1029/2007JA012610.

Vasavada, A. R., A. H. Bouchez, A. P. Ingersoll, B. Little, and C. D. Anger (1999), Jupiter's visible aurora and Io footprint, *J. Geophys. Res.*, *104*(E11), 27,133–27,142, doi:10.1029/1999JE001055.

Vogt, M. F., M. G. Kivelson, K. K. Khurana, R. J. Walker, B. Bonfond, D. Grodent, and A. Radioti (2011), Improved mapping of Jupiter's auroral features to magnetospheric sources, *J. Geophys. Res.*, *116*, A03220, doi:10.1029/2010JA016148.

  